Electronic Supplementary Material (ESI) for Dalton Transactions.

Synthesis of amphiphilic chiral salen complexes and their conformational manipulation at the air–water interface

Shigehisa Akine,*[a,b] Keisuke Nomura,[b] Mizuho Takahashi,[b] Yoko Sakata,[a,b]
Taizo Mori,* [c,d] Waka Nakanishi[c] and Katsuhiko Ariga* [c,d]

Supplementary Information

a *Nano Life Science Institute (WPI-NanoLSI), Kanazawa University, Kakuma-machi, Kanazawa 920-1192, Japan*

b *Graduate School of Natural Science and Technology, Kanazawa University, Kakuma-machi, Kanazawa 920-1192, Japan*

c *Research Center for Materials Nanoarchitectonics (WPI-MANA), National Institute for Materials Science (NIMS), 1-1 Namiki, Tsukuba, Ibaraki 305-0044, Japan*

d *Graduate School of Frontier Sciences, The University of Tokyo, 5-1-5 Kashiwanoha, Kashiwa, Chiba 277-8561, Japan*

1. Synthesis of aldehydes A1 and A2.

1.1. Synthesis of carboxylic acid 1.

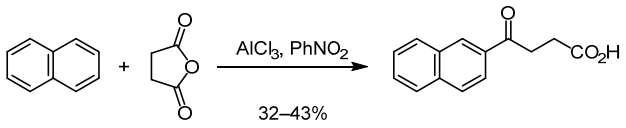

1

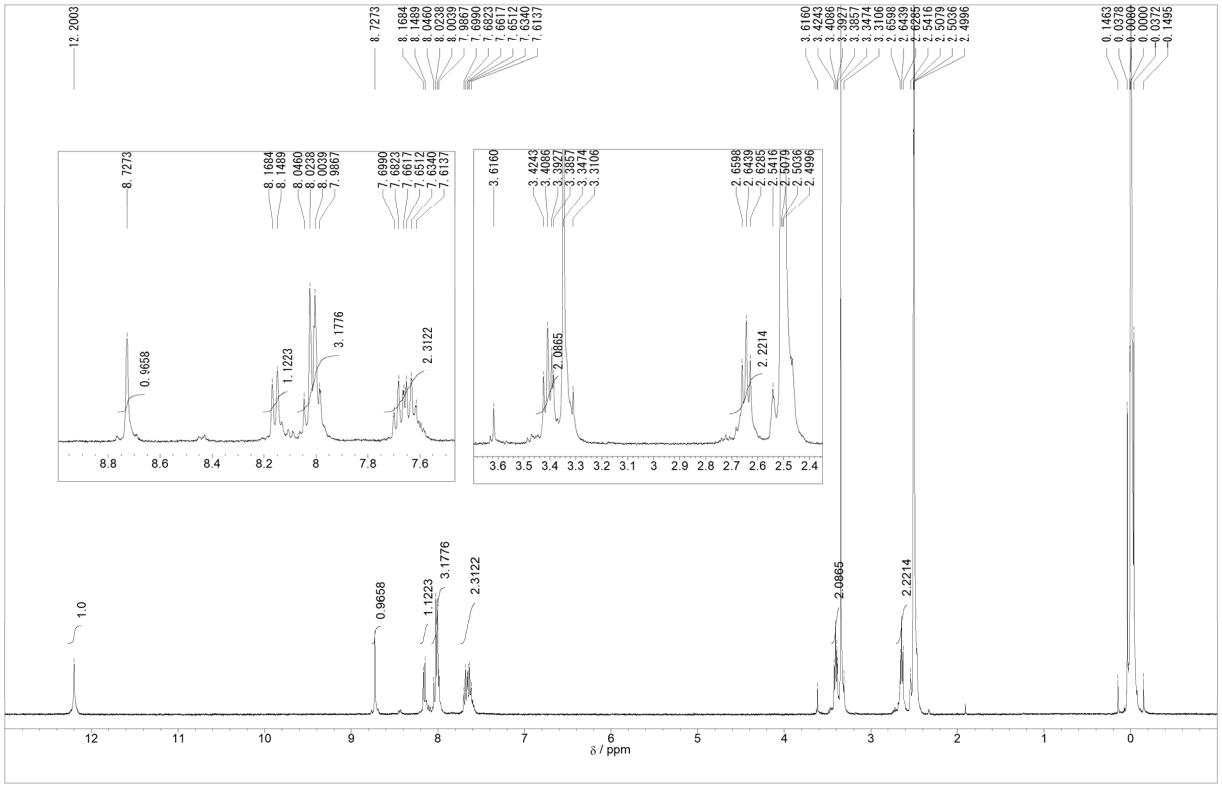

Figure S1. ^{1}H NMR spectrum of compound **1** (400 MHz, $CDCl_3$).

1.2. Synthesis of carboxylic acid 2.

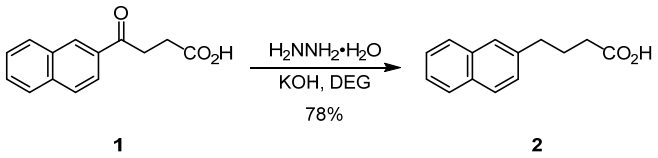

1 2

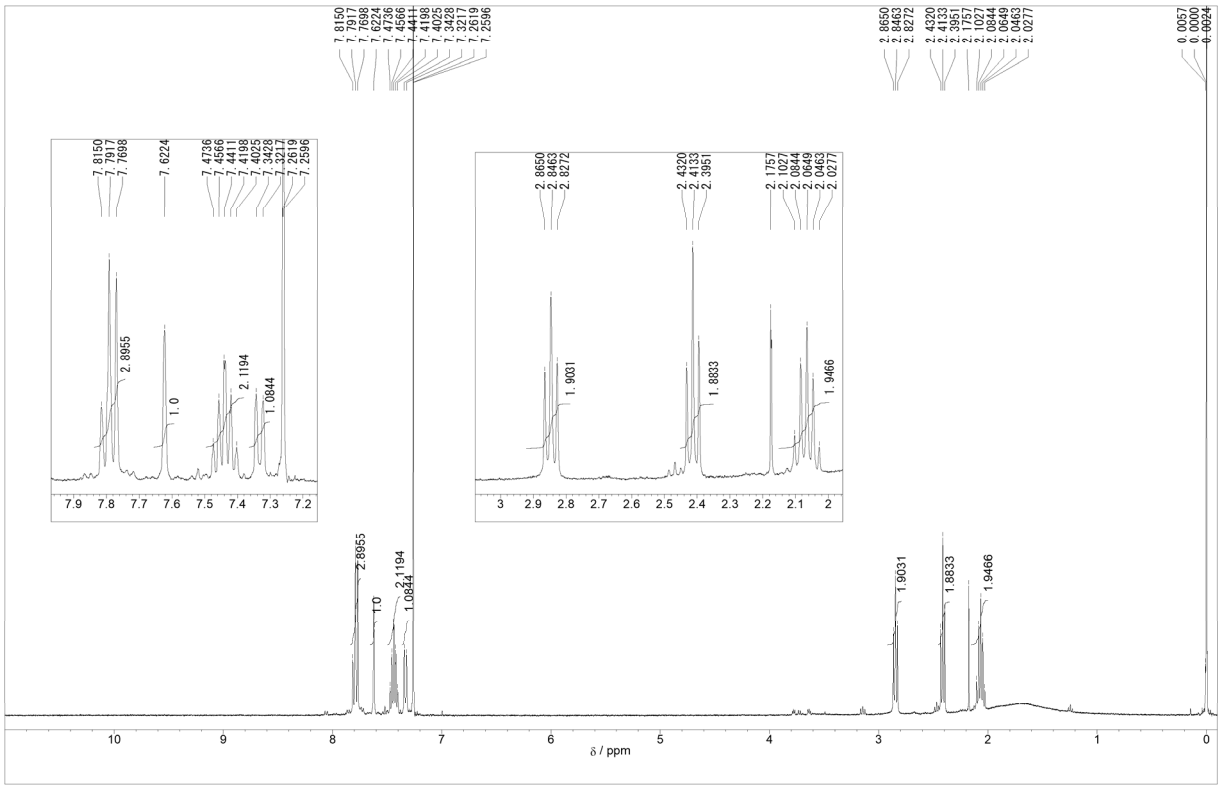

Figure S2. ^{1}H NMR spectrum of compound **2** (400 MHz, $CDCl_3$).

1.3. Synthesis of ketone 3.

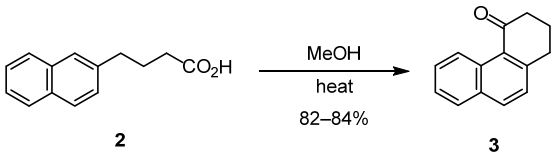

2 **3**

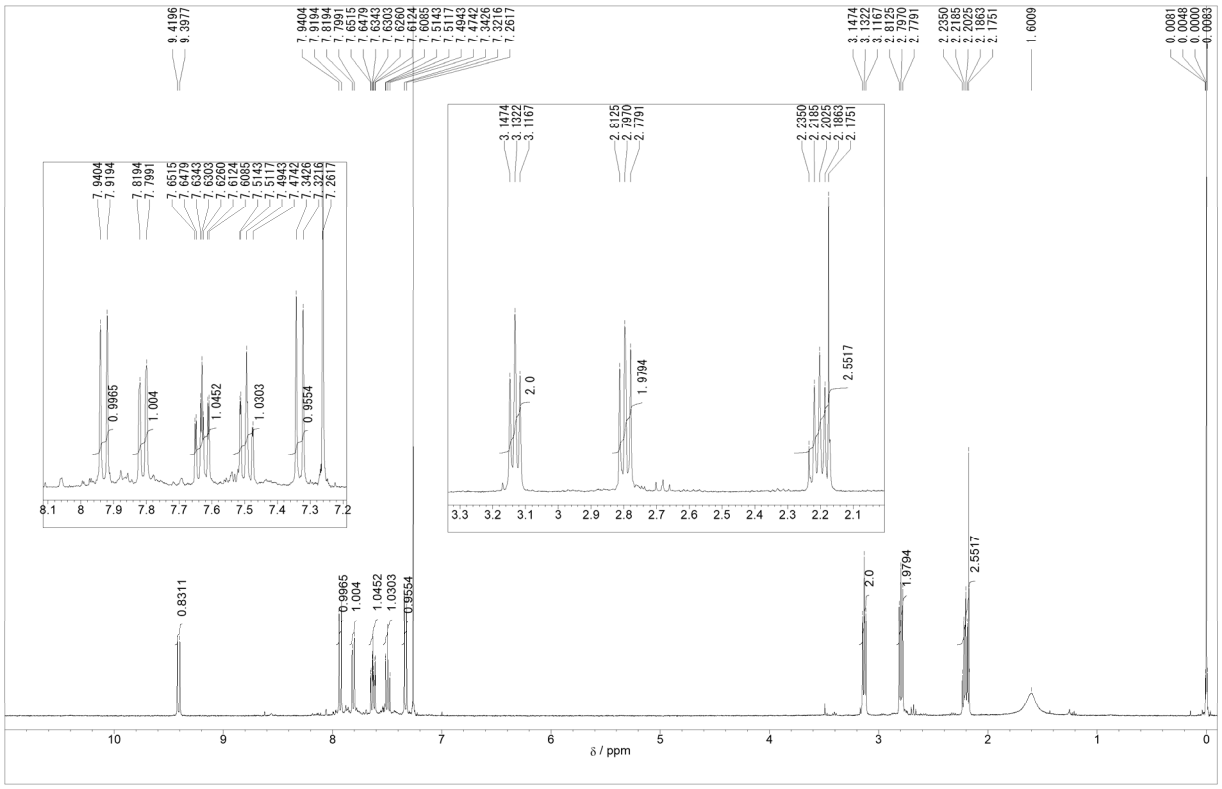

Figure S3. ^{1}H NMR spectrum of compound **3** (400 MHz, $CDCl_3$).

1.4. Synthesis of compound 4.

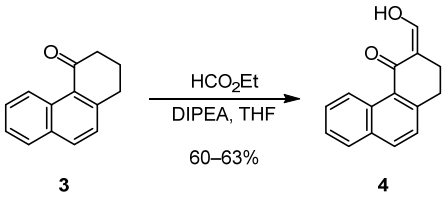

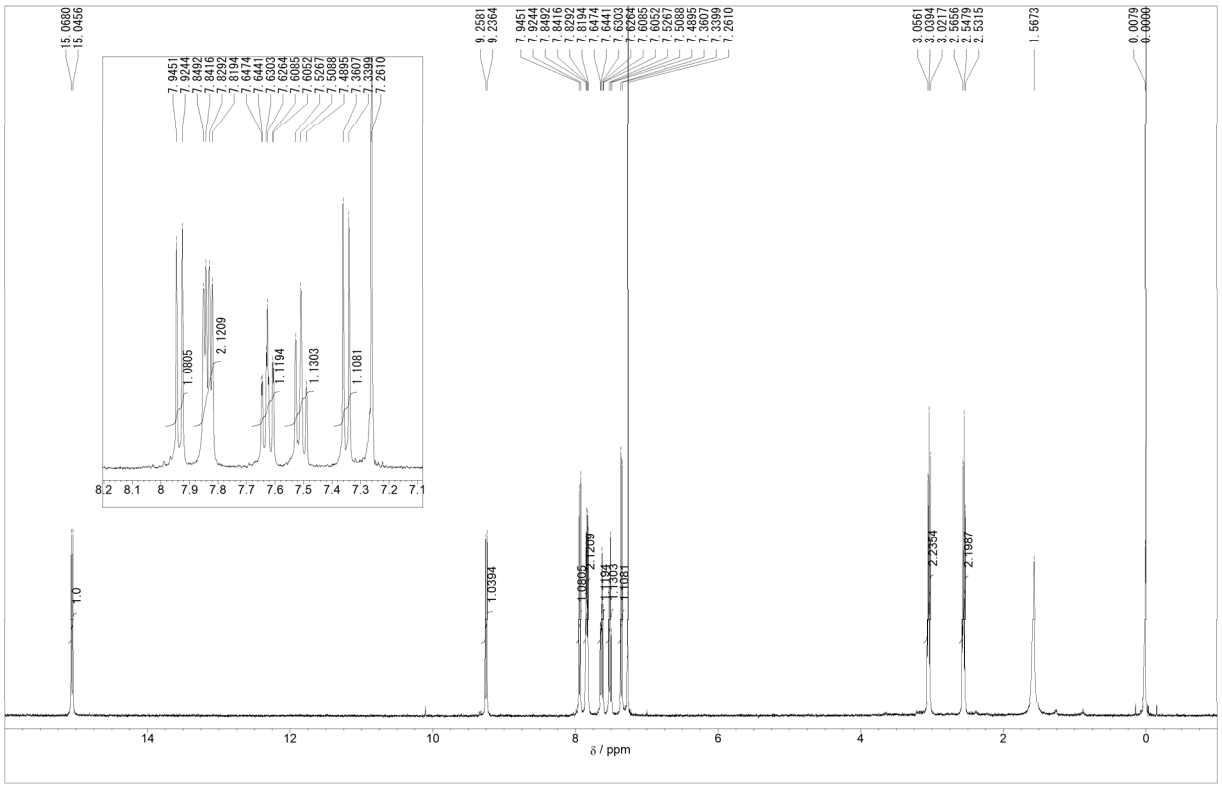

Figure S4. ^{1}H NMR spectrum of compound **4** (400 MHz, $CDCl_3$).

1.5. Synthesis of A1.[1]

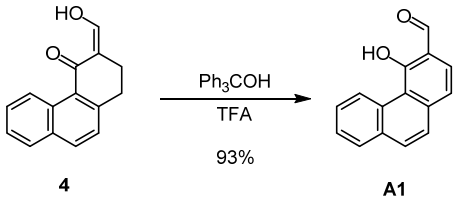

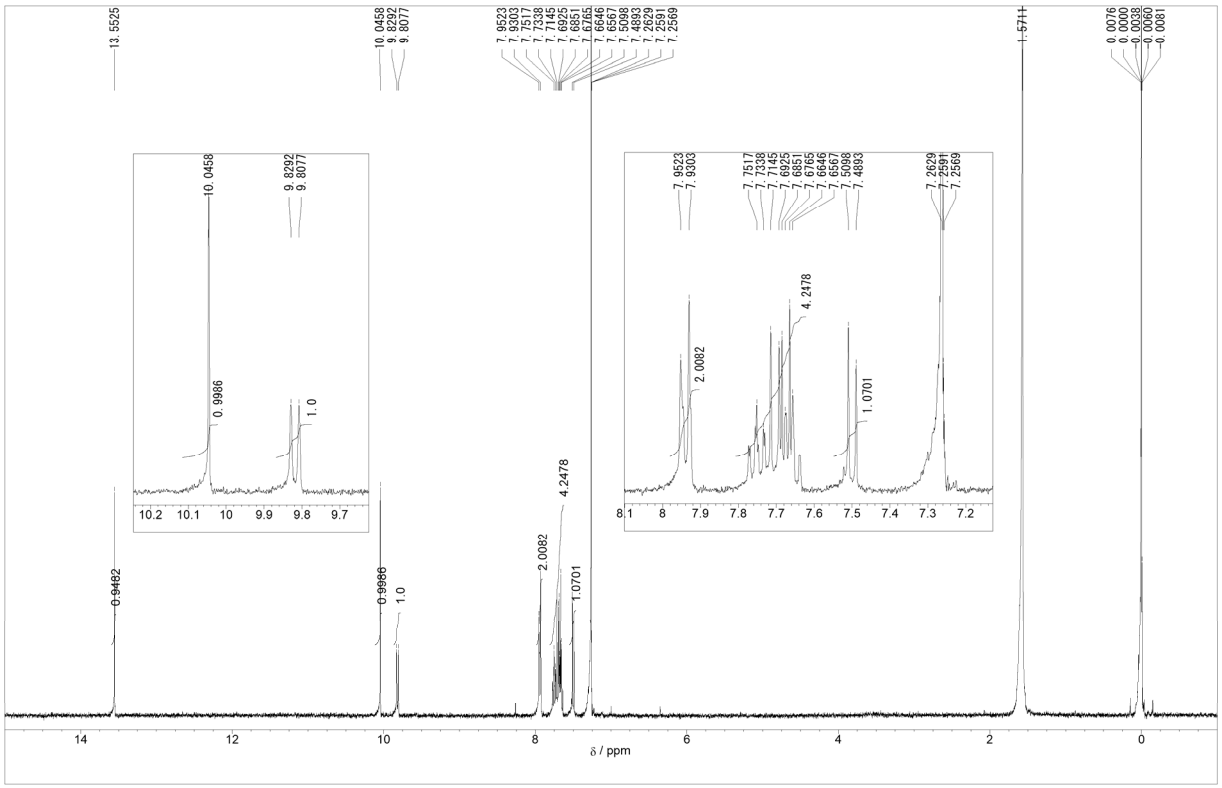

Figure S5. ^{1}H NMR spectrum of compound **A1** (400 MHz, $CDCl_3$).

[1] (a) A. V. Wiznycia, J. Desper, C. J. Levy, *Chem. Commun.*, **2005**, 4693–4695; (b) M. W. van der Meijden, E. Gelens, N. M. Quirós, J. D. Fuhr, J. E. Gayone, H. Ascolani, K. Wurst, M. Lingenfelder, R. M. Kellogg, *Chem. Eur. J.*, 2016, **22**, 1484–1492; (c) N. Harada, A. Saito, N. Koumura, H. Uda, B. de Lange, W. F. Jager, H. Wynberg, B. L. Feringa, *J. Am. Chem. Soc.*, 1997, **119**, 7241–7248.

1.6. Synthesis of 1-hydroxy-2-naphthalaldehyde (A2).[2]

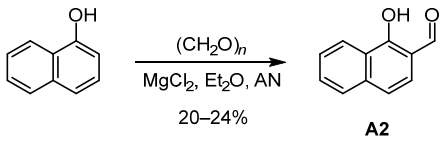

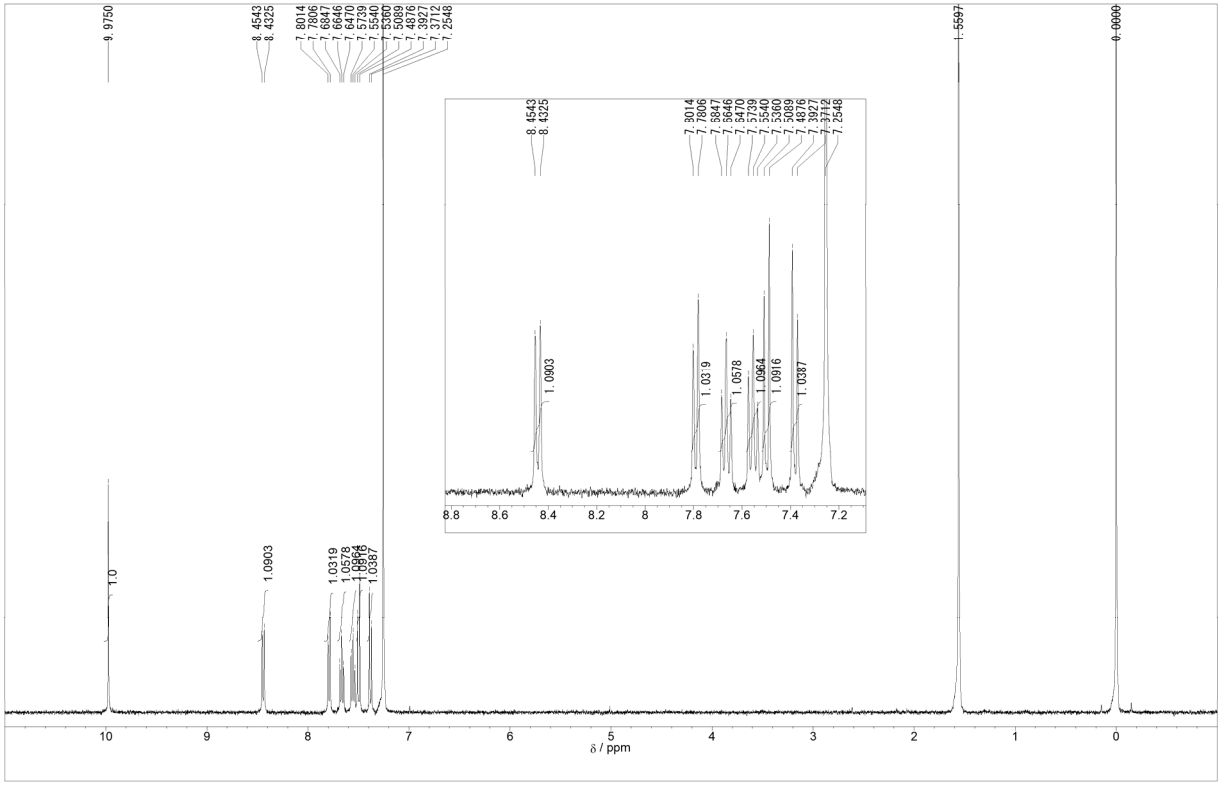

Figure S6. ^{1}H NMR spectrum of compound **A2** (400 MHz, $CDCl_3$).

[2] C. J. Lim, J. Y. Choi, B. H. Lee, K.-S. Oh, K. Y. Yi, *Chem. Pharm. Bull.*, 2013, **61**, 1239–1247.

2. Synthesis of amphiphilic chiral salen ligands $H_2L^{1a,b}$ and $H_2L^{2a,b}$.

2.1. ^1H and ^{13}C NMR spectra of 2a.

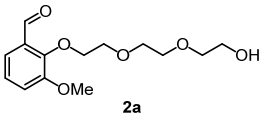

2a

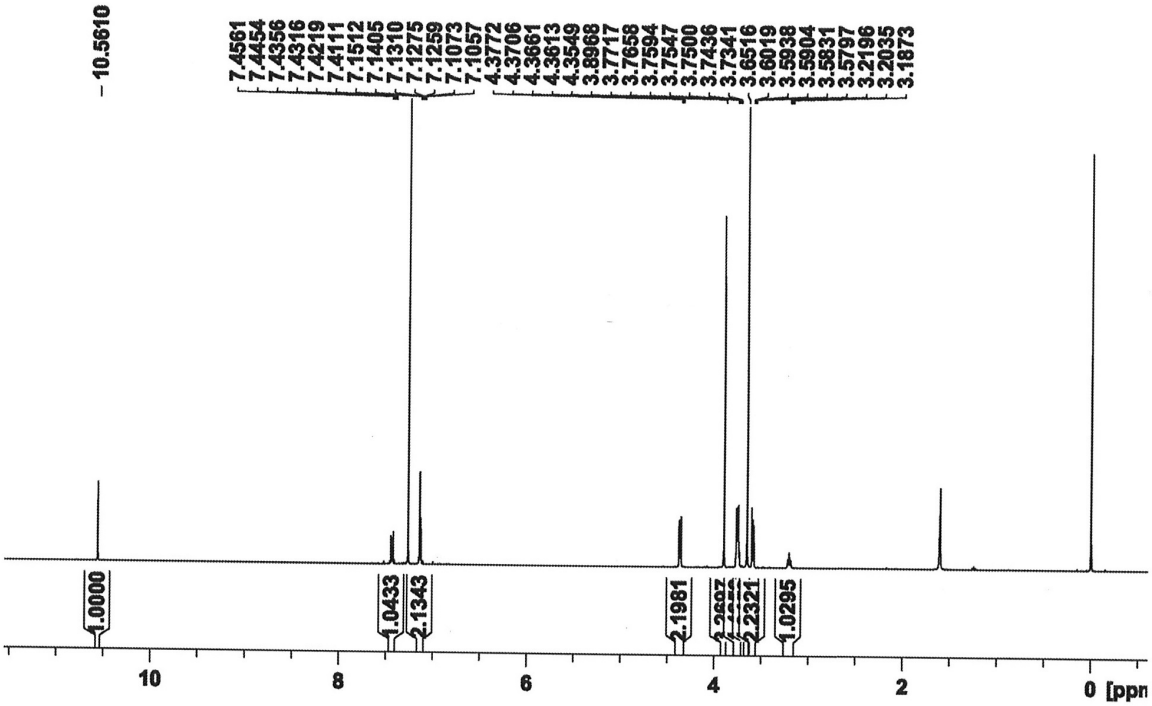

Figure S7. ^1H NMR spectrum of compound **2a** (400 MHz, $CDCl_3$).

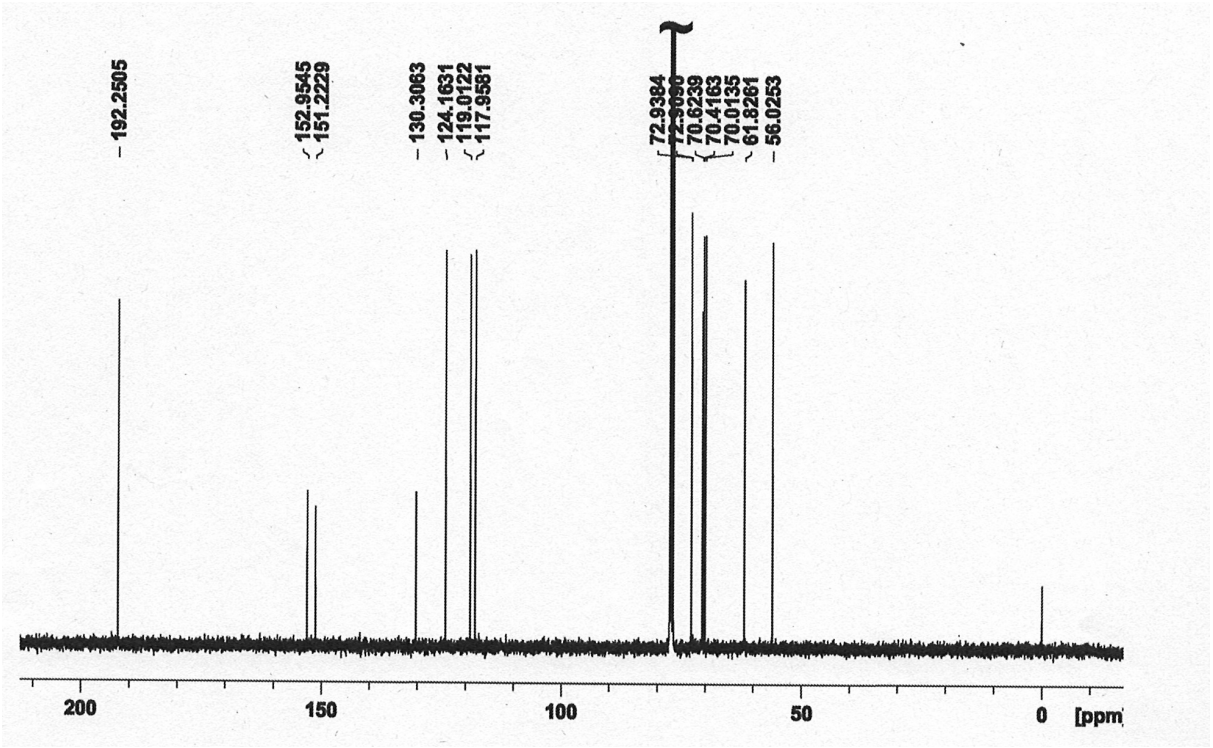

Figure S8. ^{13}C NMR spectrum of compound **2a** (100 MHz, $CDCl_3$).

2.2. ^{1}H and ^{13}C NMR spectra of 2b.

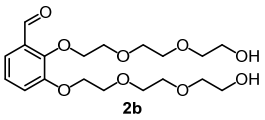

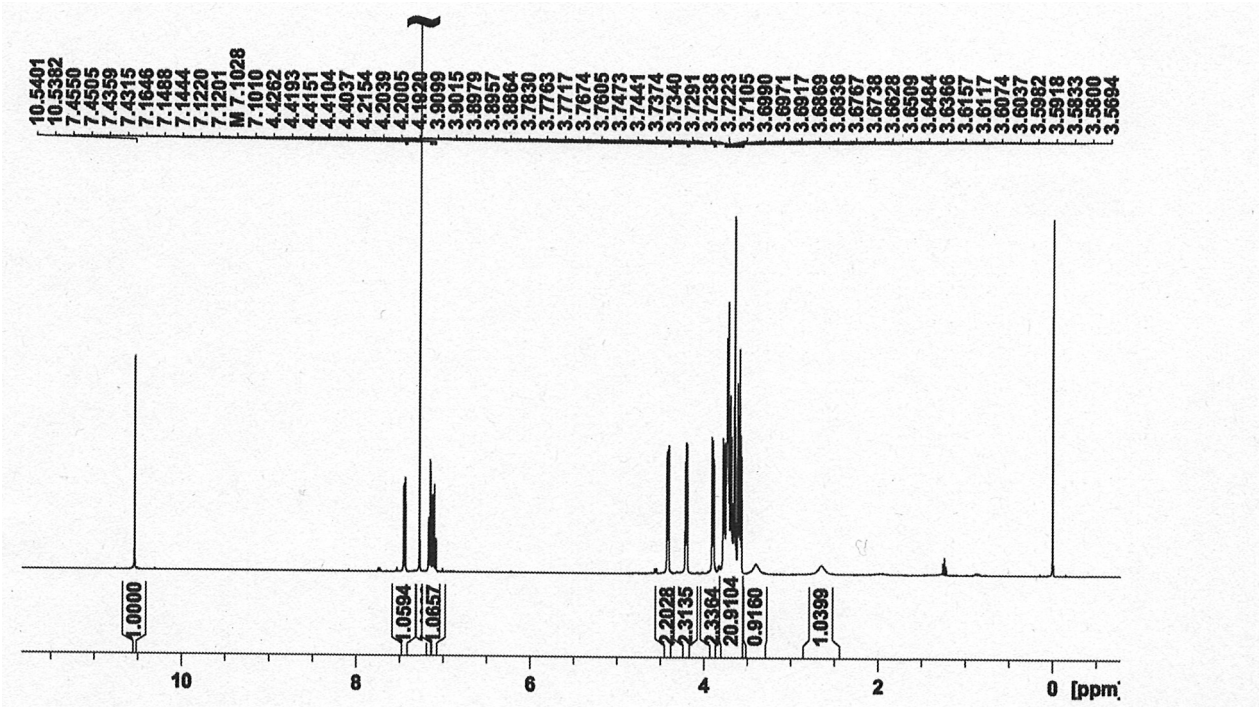

Figure S9. ^{1}H NMR spectrum of compound **2b** (400 MHz, $CDCl_3$).

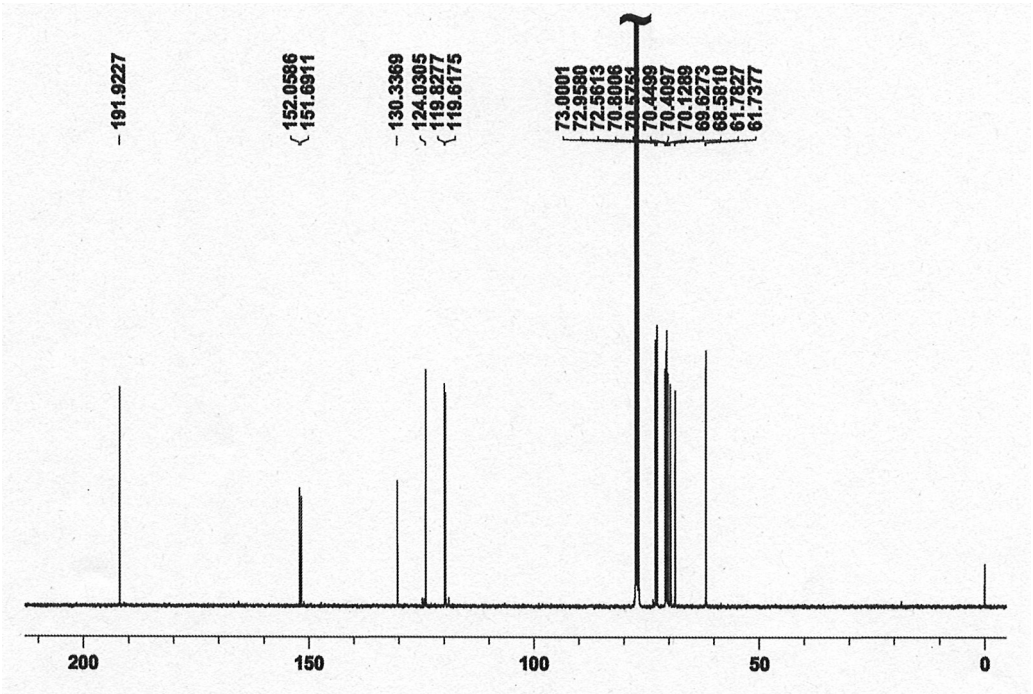

Figure S10. ^{13}C NMR spectrum of compound **2b** (100 MHz, $CDCl_3$).

2.3. ^{1}H and ^{13}C NMR spectra of 3a.

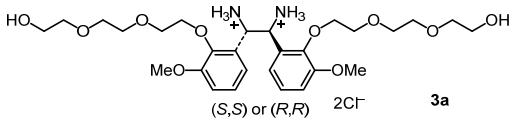

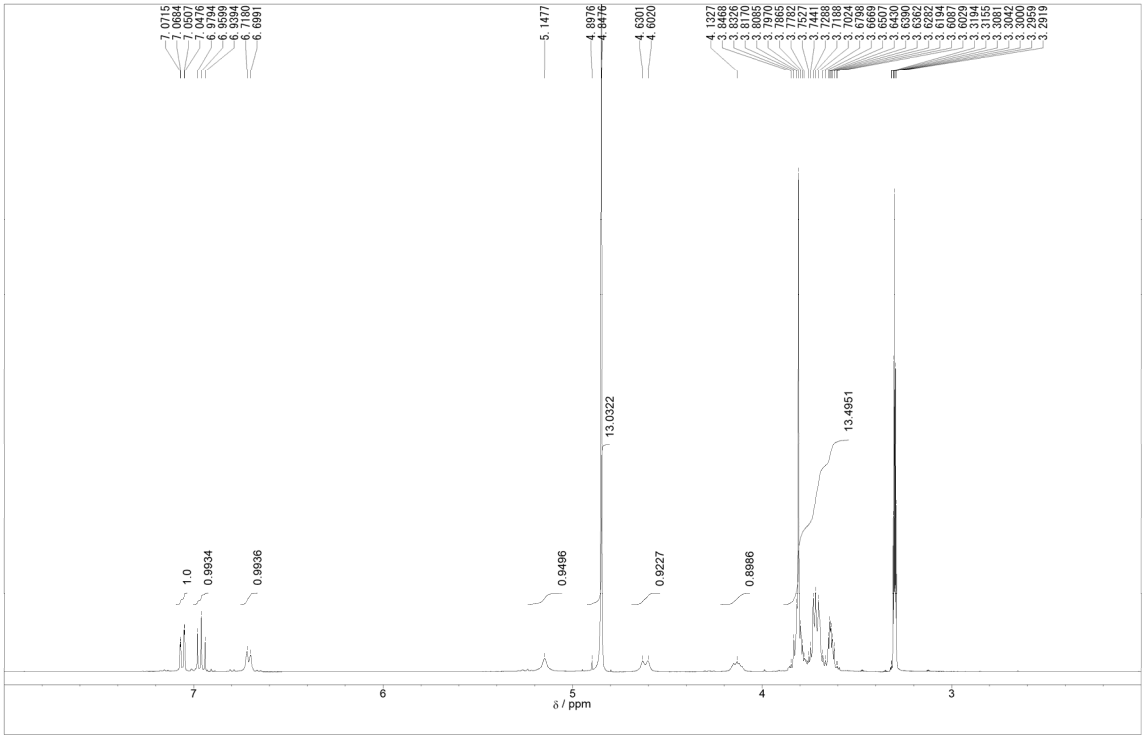

Figure S11. ^{1}H NMR spectrum of compound **3a** (400 MHz, $CDCl_3$).

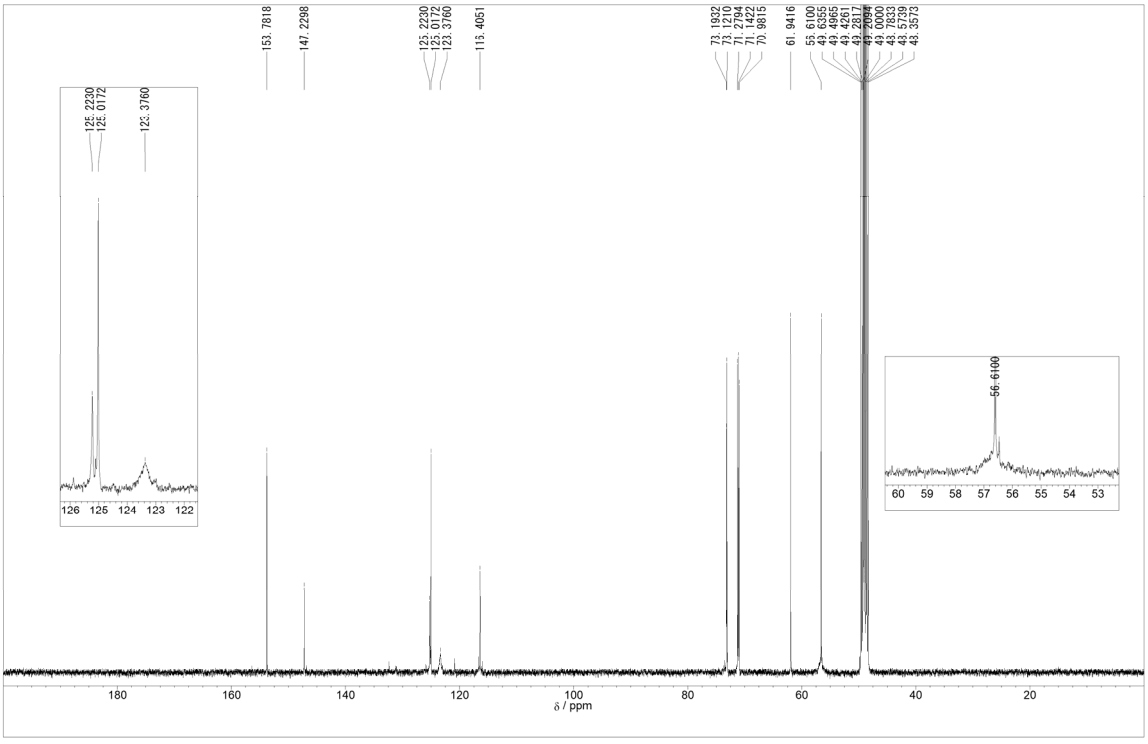

Figure S12. ^{13}C NMR spectrum of compound **3a** (100 MHz, $CDCl_3$).

2.4. ^{1}H and ^{13}C NMR spectra of 3b.

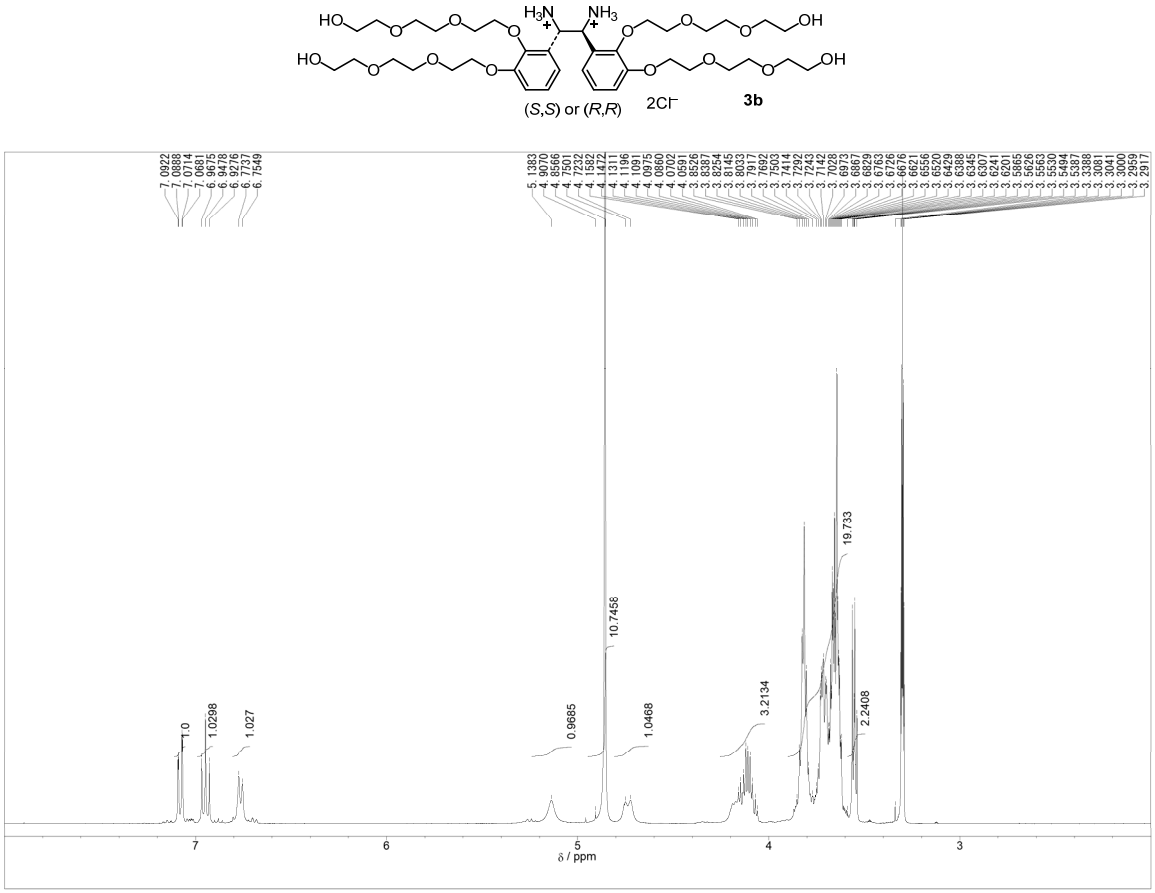

Figure S13. ^{1}H NMR spectrum of compound **3b** (400 MHz, $CDCl_3$).

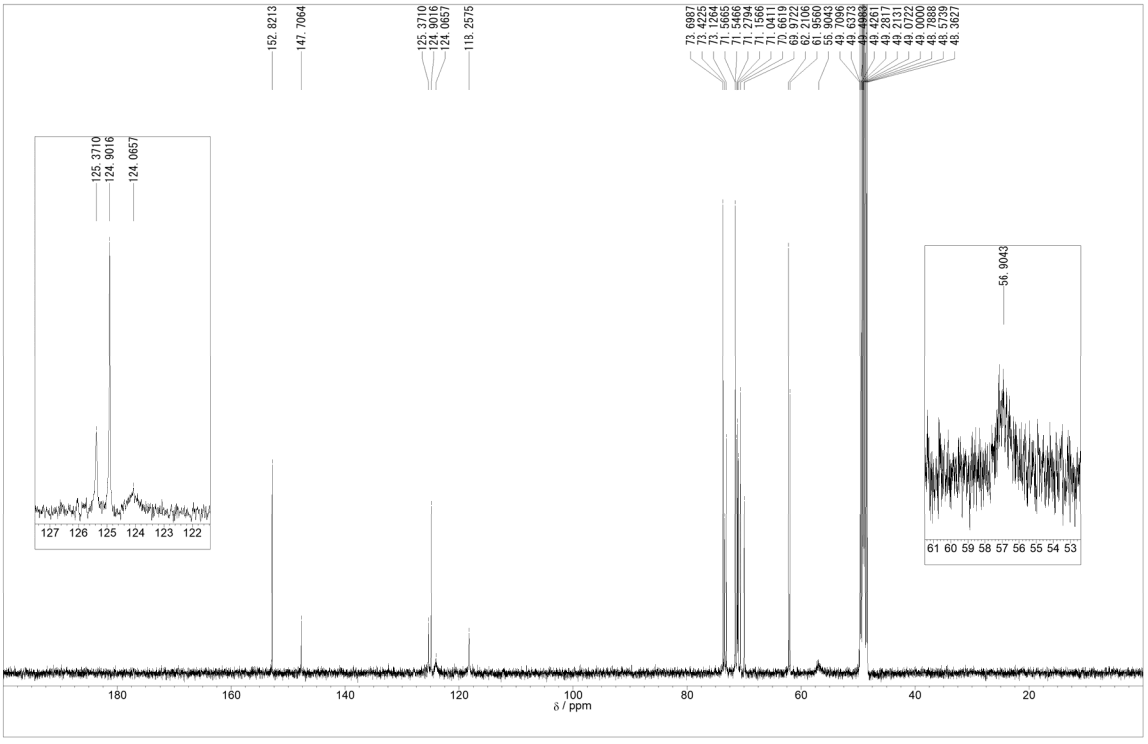

Figure S14. ^{13}C NMR spectrum of compound **3b** (100 MHz, $CDCl_3$).

2.5. ^{1}H and ^{13}C NMR spectra of H_2L^{1a}.

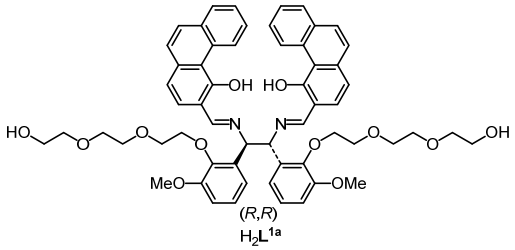

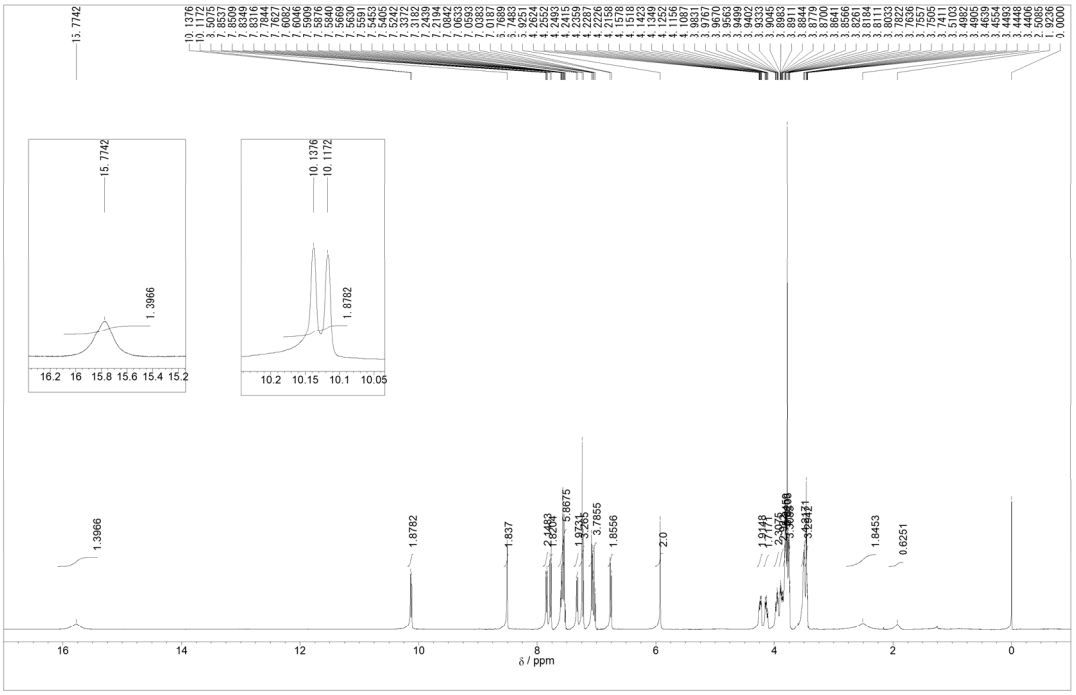

Figure S15. ^{1}H NMR spectrum of amphiphilic chiral salen ligand H_2L^{1a} (400 MHz, $CDCl_3$).

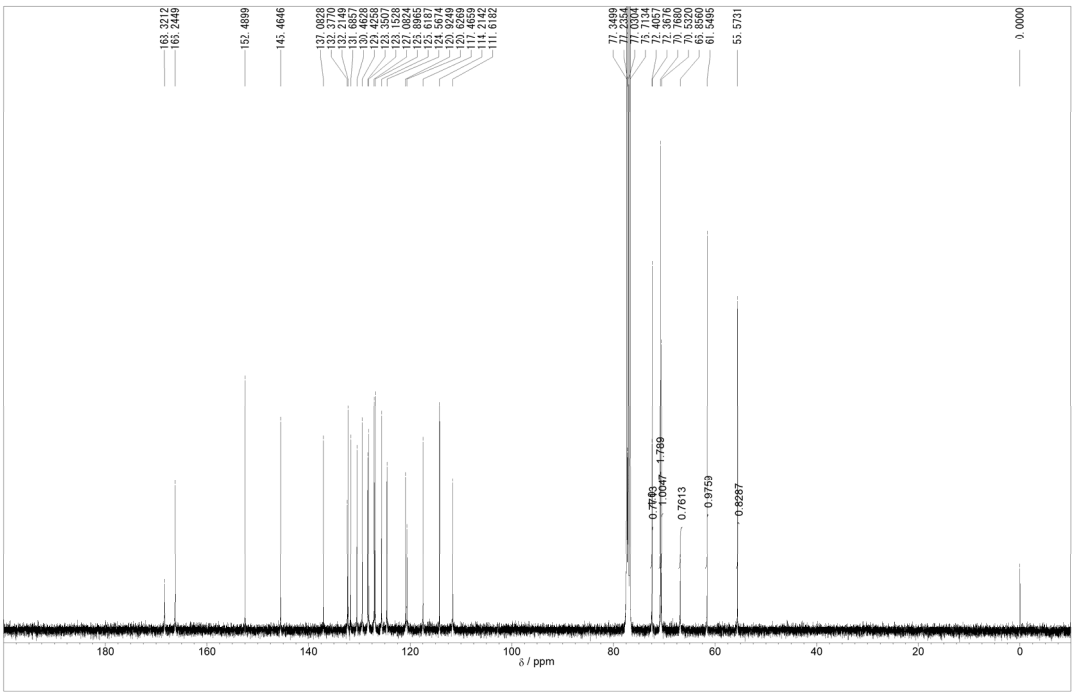

Figure S16. ^{13}C NMR spectrum of amphiphilic chiral salen ligand H_2L^{1a} (100 MHz, $CDCl_3$).

2.6. ^{1}H and ^{13}C NMR spectra of H_2L^{1b}.

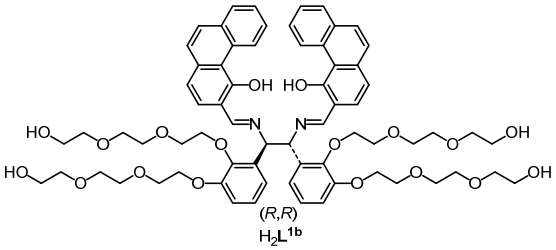

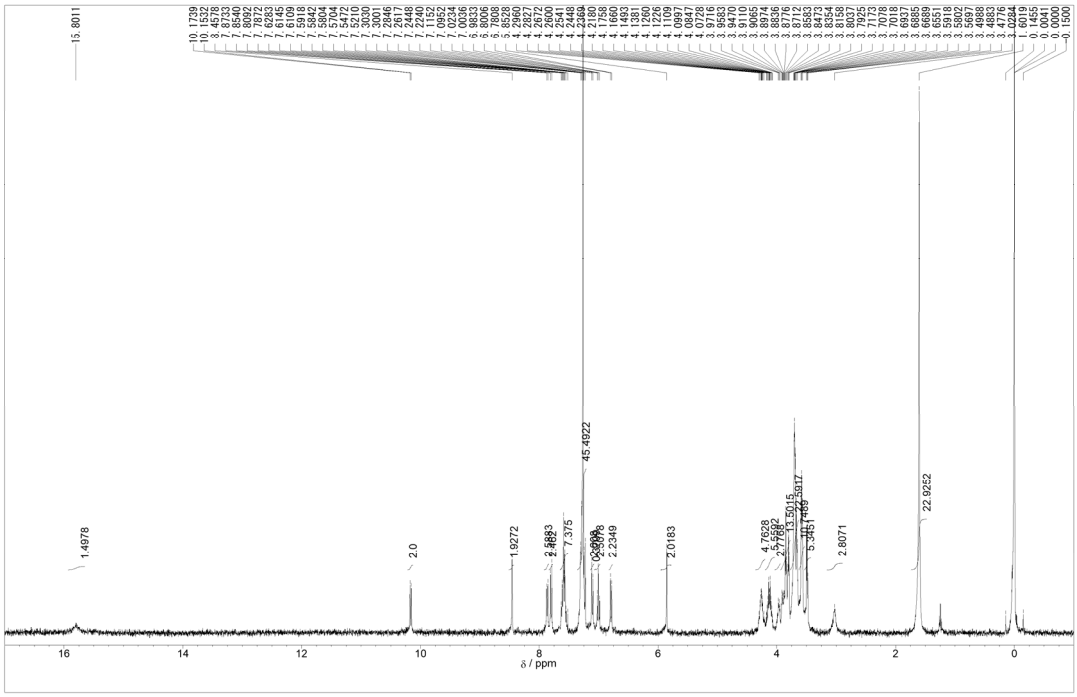

Figure S17. ^{1}H NMR spectrum of amphiphilic chiral salen ligand $H_2\mathbf{L^{1b}}$ (400 MHz, $CDCl_3$).

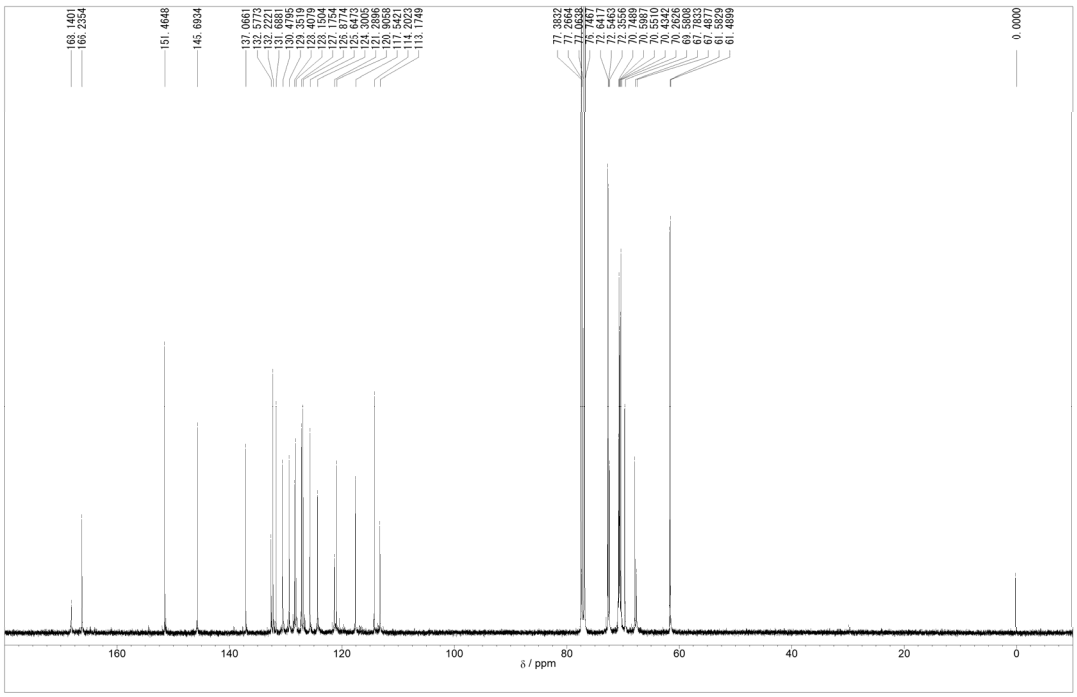

Figure S18. ^{13}C NMR spectrum of amphiphilic chiral salen ligand $H_2\mathbf{L^{1b}}$ (100 MHz, $CDCl_3$).

2.7. ^{1}H and ^{13}C NMR spectra of H_2L^{2a}.

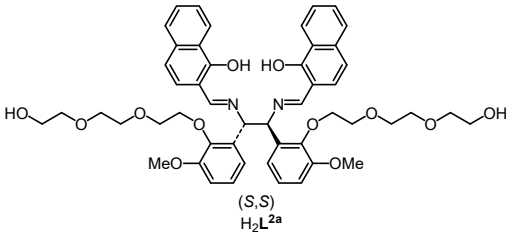

(*S*,*S*)
H_2L^{2a}

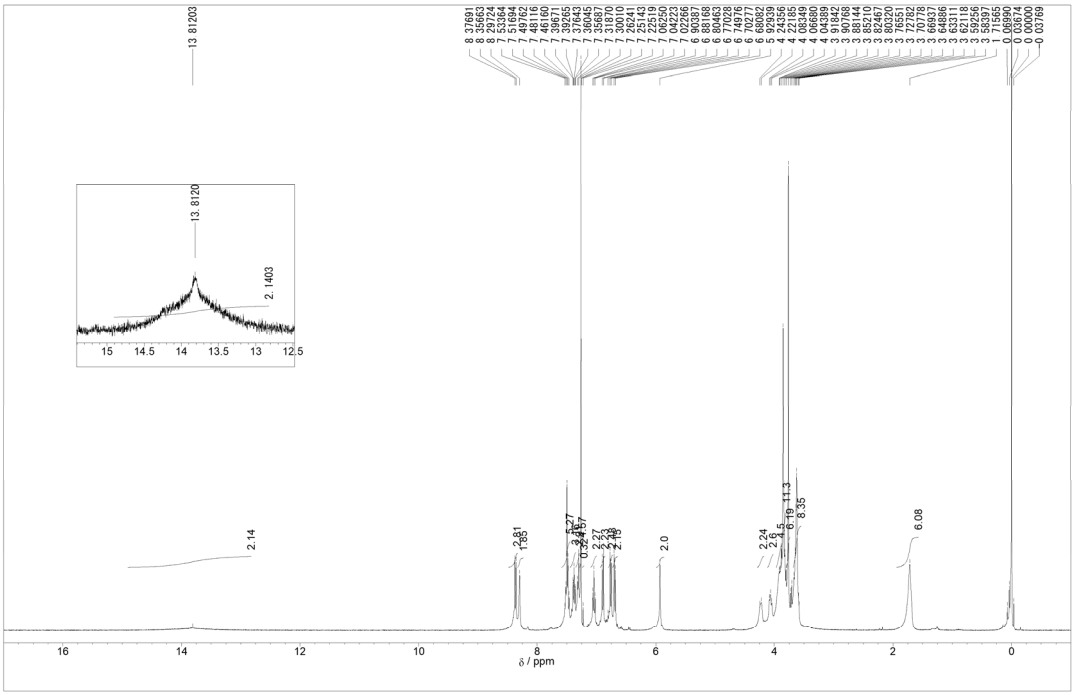

Figure S19. ^{1}H NMR spectrum of amphiphilic chiral salen ligand $H_2\mathbf{L^{2a}}$ (400 MHz, $CDCl_3$).

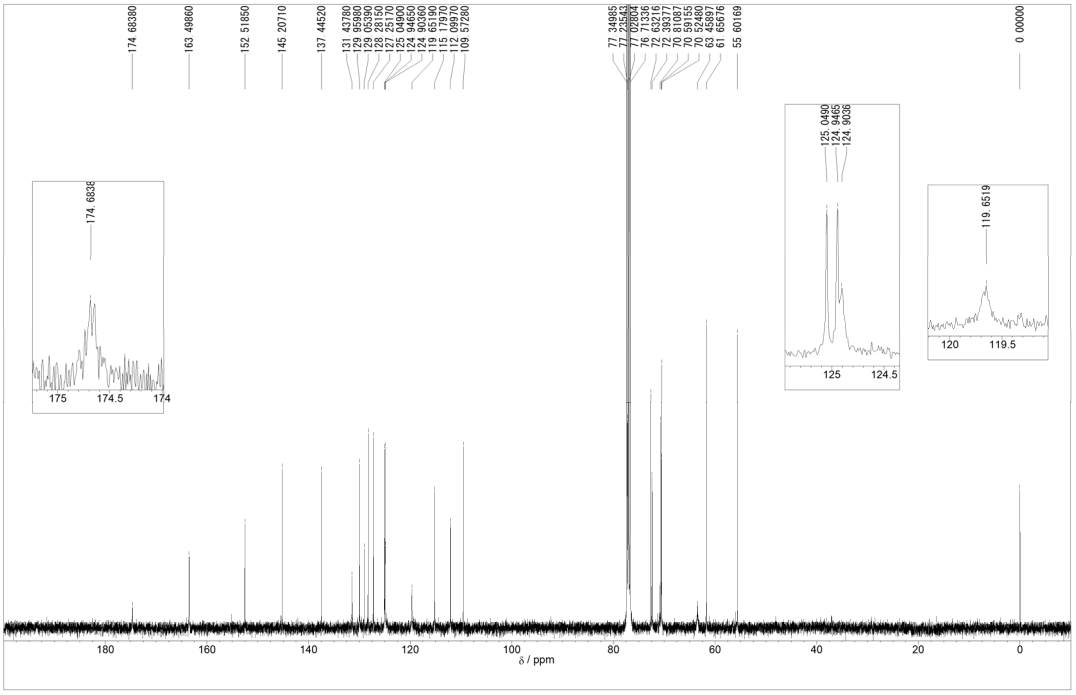

Figure S20. ^{13}C NMR spectrum of amphiphilic chiral salen ligand $H_2\mathbf{L^{2a}}$ (100 MHz, $CDCl_3$).

2.8. ^{1}H and ^{13}C NMR spectra of H_2L^{2b}.

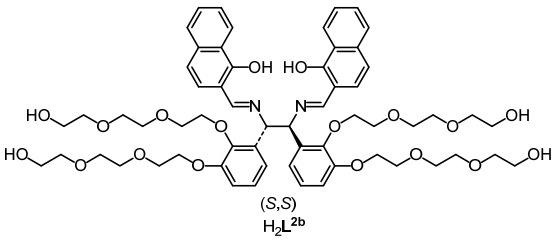

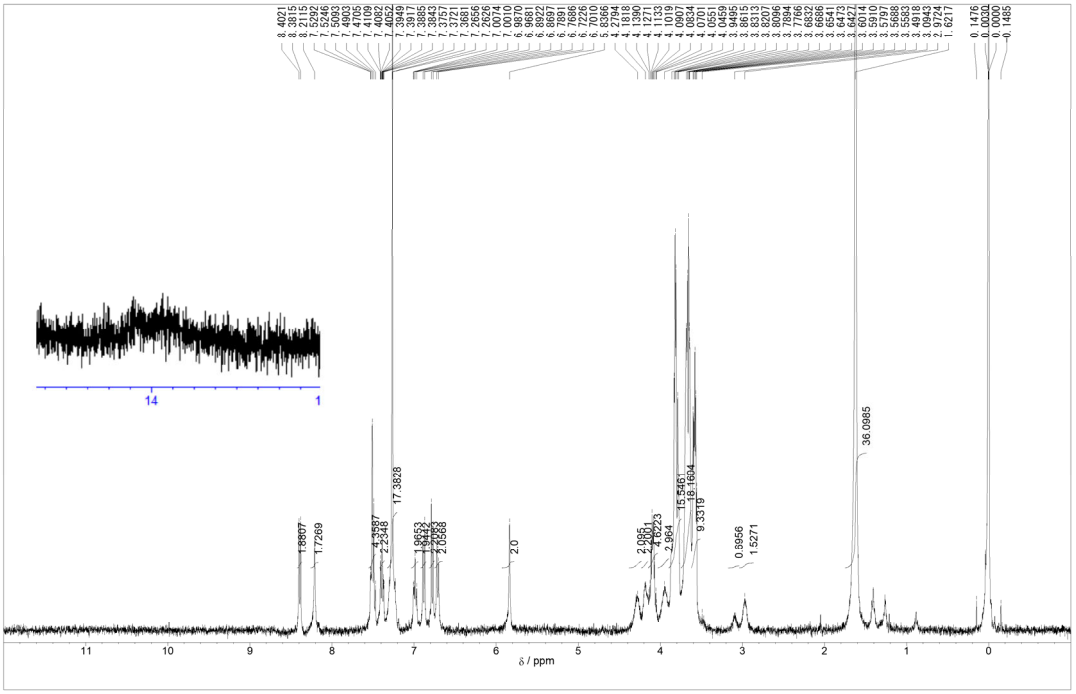

Figure S21. ^{1}H NMR spectrum of amphiphilic chiral salen ligand $H_2\mathbf{L^{2b}}$ (400 MHz, $CDCl_3$).

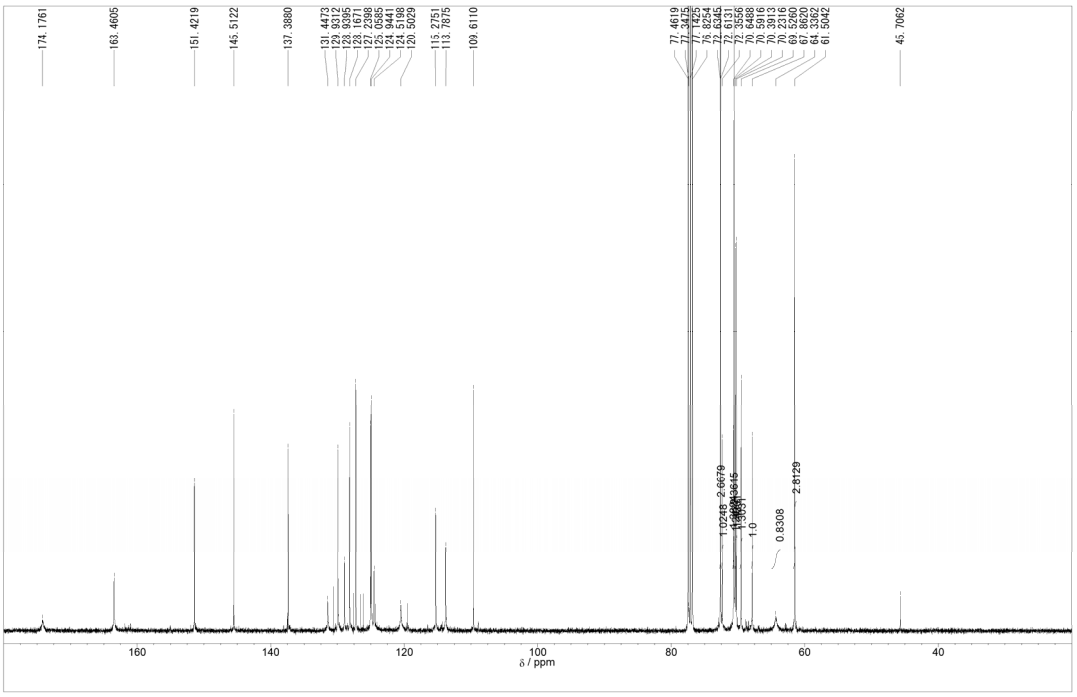

Figure S22. ^{13}C NMR spectrum of amphiphilic chiral salen ligand $H_2\mathbf{L^{2b}}$ (100 MHz, $CDCl_3$).

3. Synthesis of amphiphilic chiral salen metal complexes.

3.1. ^{1}H NMR spectrum of [L^{1a}Ni].

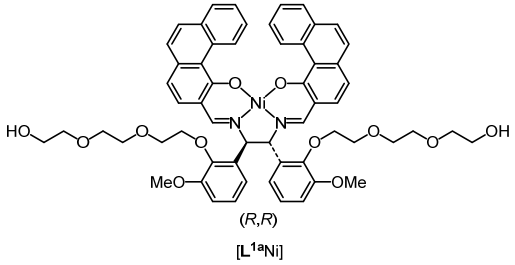

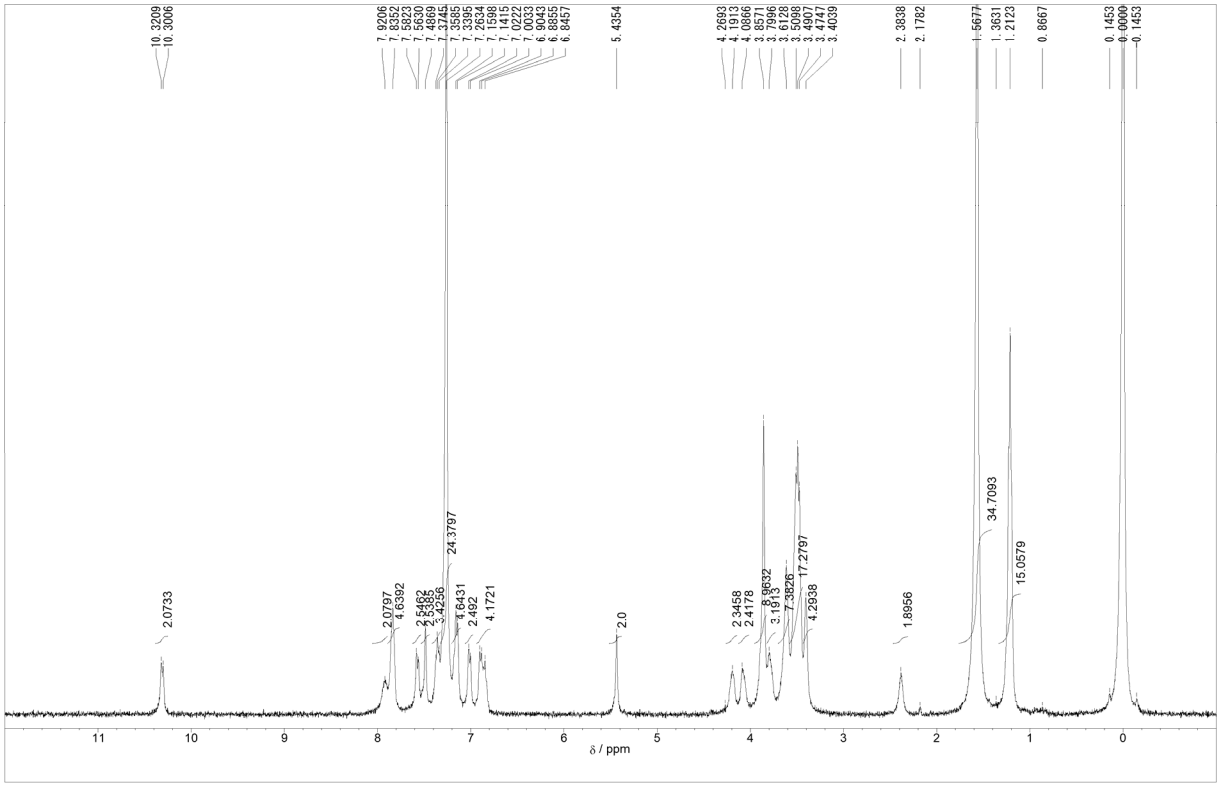

Figure S23. ^{1}H NMR spectrum of amphiphilic chiral salen complex [**L^{1a}**Ni] (400 MHz, $CDCl_3$).

3.2. ^{1}H NMR spectrum of [L^{1b}Ni].

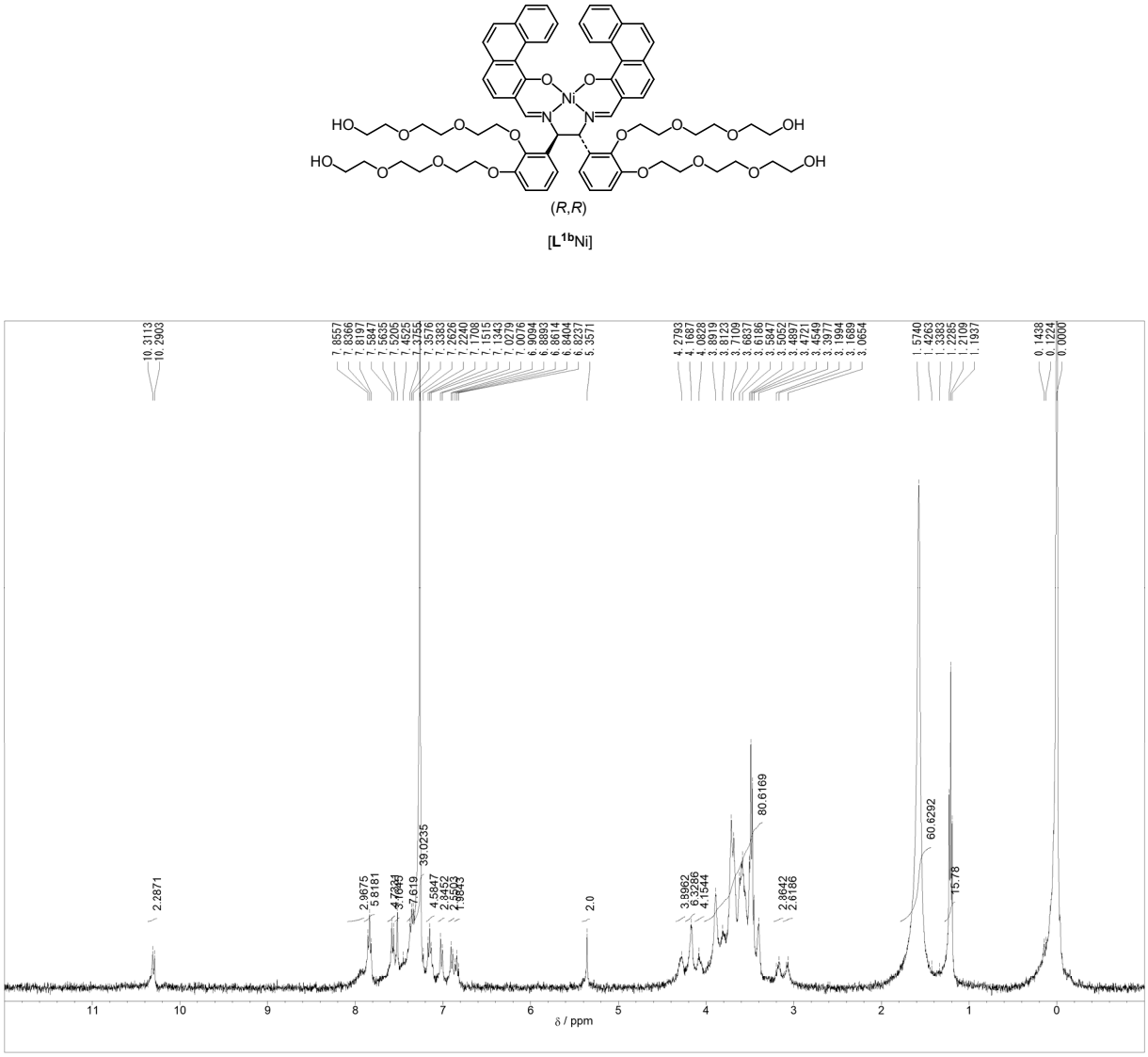

Figure S24. ^{1}H NMR spectrum of amphiphilic chiral salen complex [**L^{1b}**Ni] (400 MHz, $CDCl_3$).

3.3. ^{1}H NMR spectrum of [L^{2a}Ni].

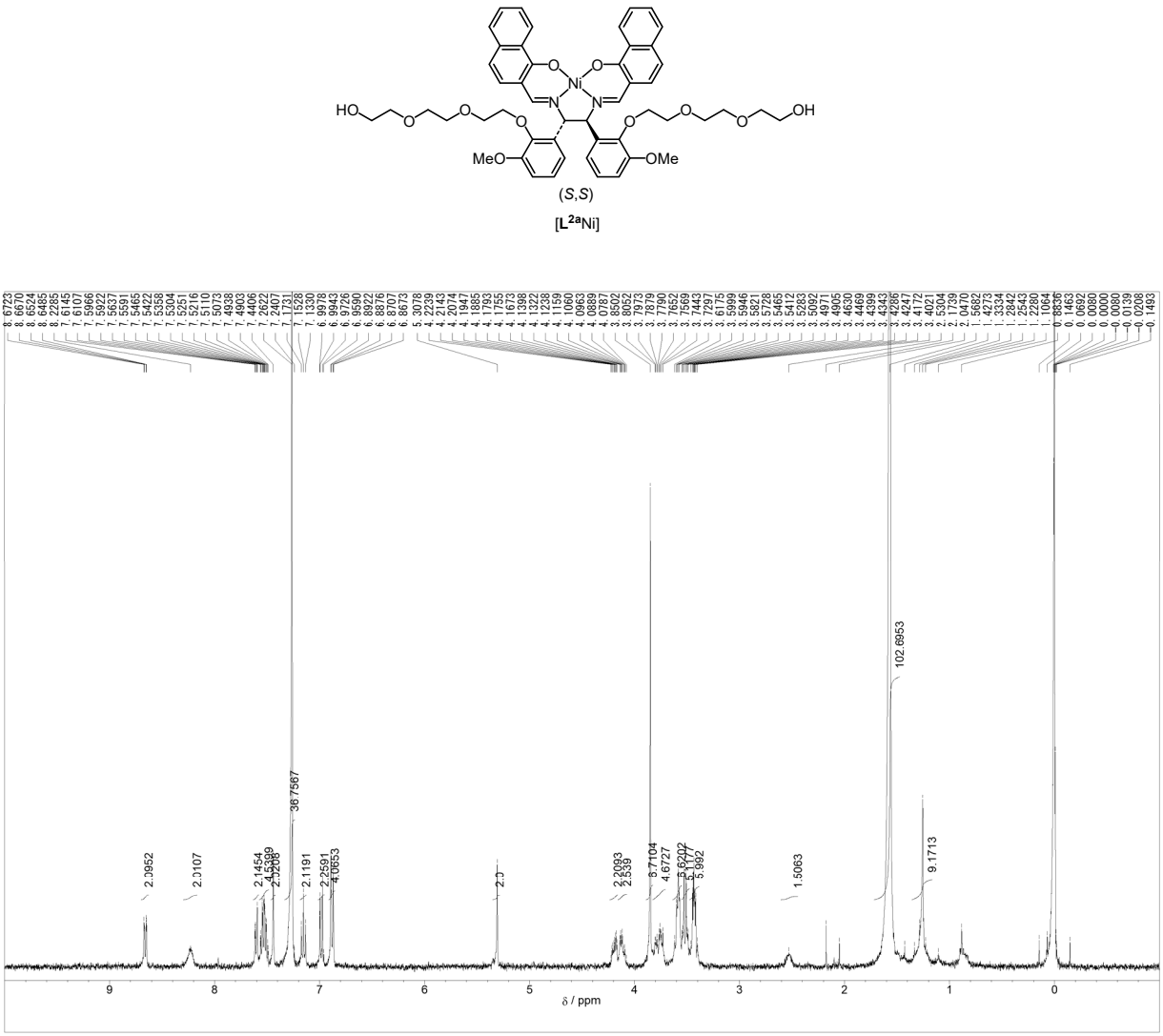

Figure S25. ^{1}H NMR spectrum of amphiphilic chiral salen complex [**L^{2a}Ni**] (400 MHz, $CDCl_3$).

3.4. ^{1}H NMR spectrum of [L^{2b}Ni].

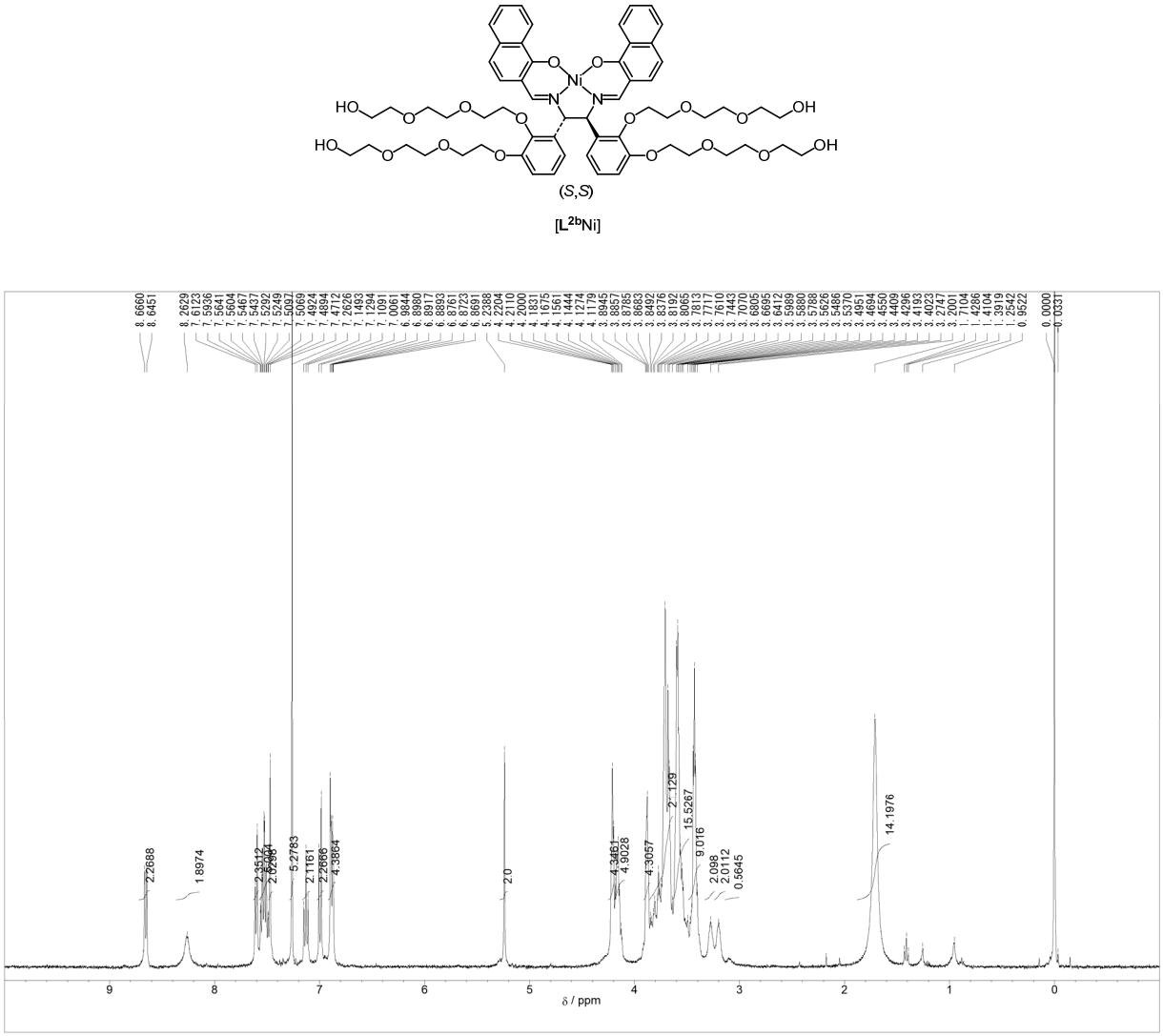

Figure S26. ^{1}H NMR spectrum of amphiphilic chiral salen complex [**L^{2b}Ni**] (400 MHz, $CDCl_3$).

3.5. ^{1}H NMR spectrum of [L^{1b}Cu].

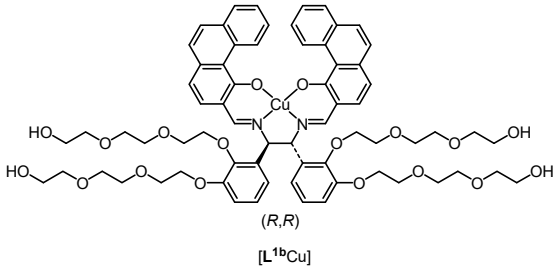

[L^{1b}Cu]

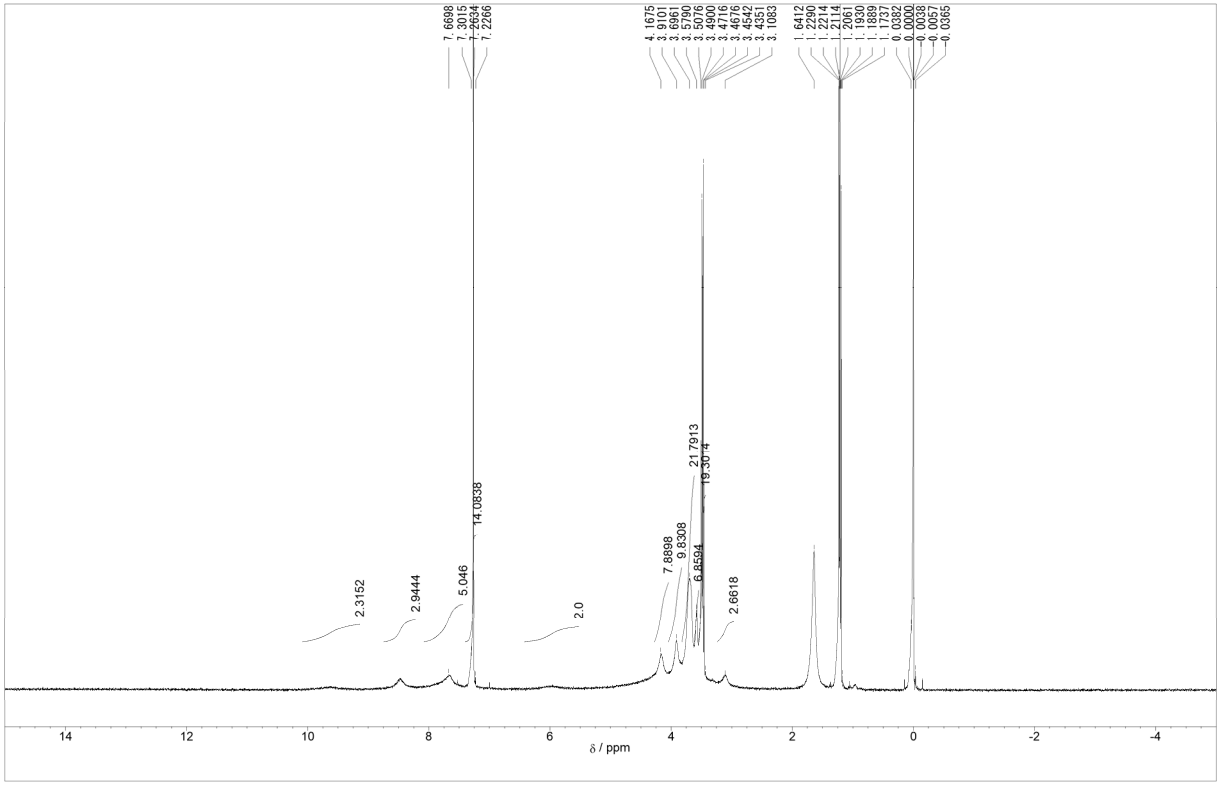

Figure S27. ^{1}H NMR spectrum of amphiphilic chiral salen complex [**L^{1b}**Cu] (400 MHz, $CDCl_3$).

3.6. ^{1}H NMR spectrum of [L^{1b}Co(MeNH$_2$)$_2$](OTf).

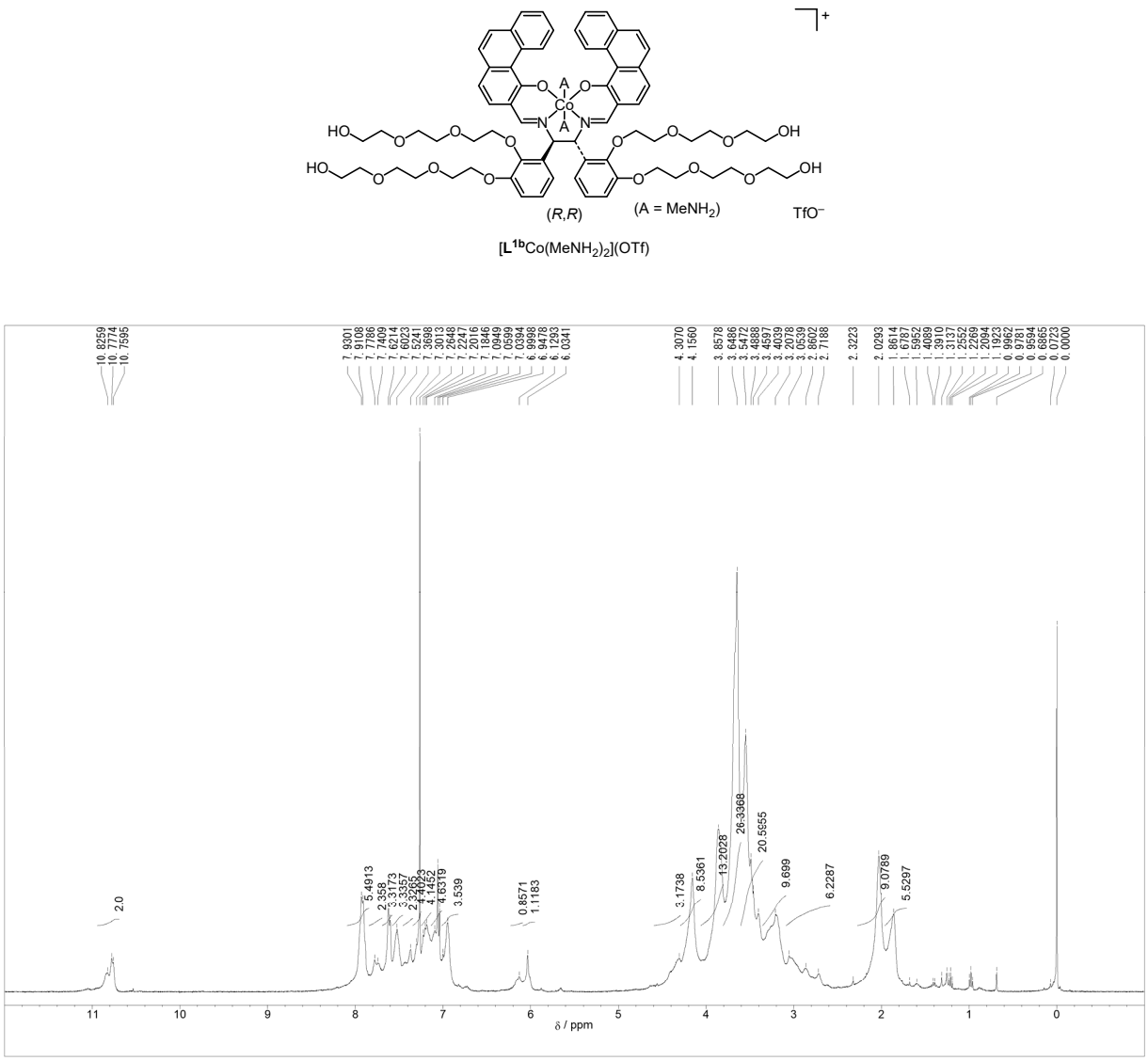

Figure S28. ^{1}H NMR spectrum of amphiphilic chiral salen complex [**L^{1b}**Co(MeNH$_2$)$_2$](OTf) (400 MHz, $CDCl_3$).

3.7. ^{1}H NMR spectrum of [L^{1b}Zn].

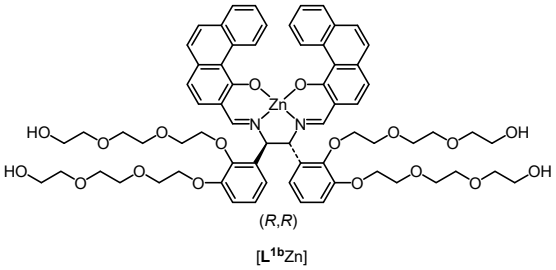

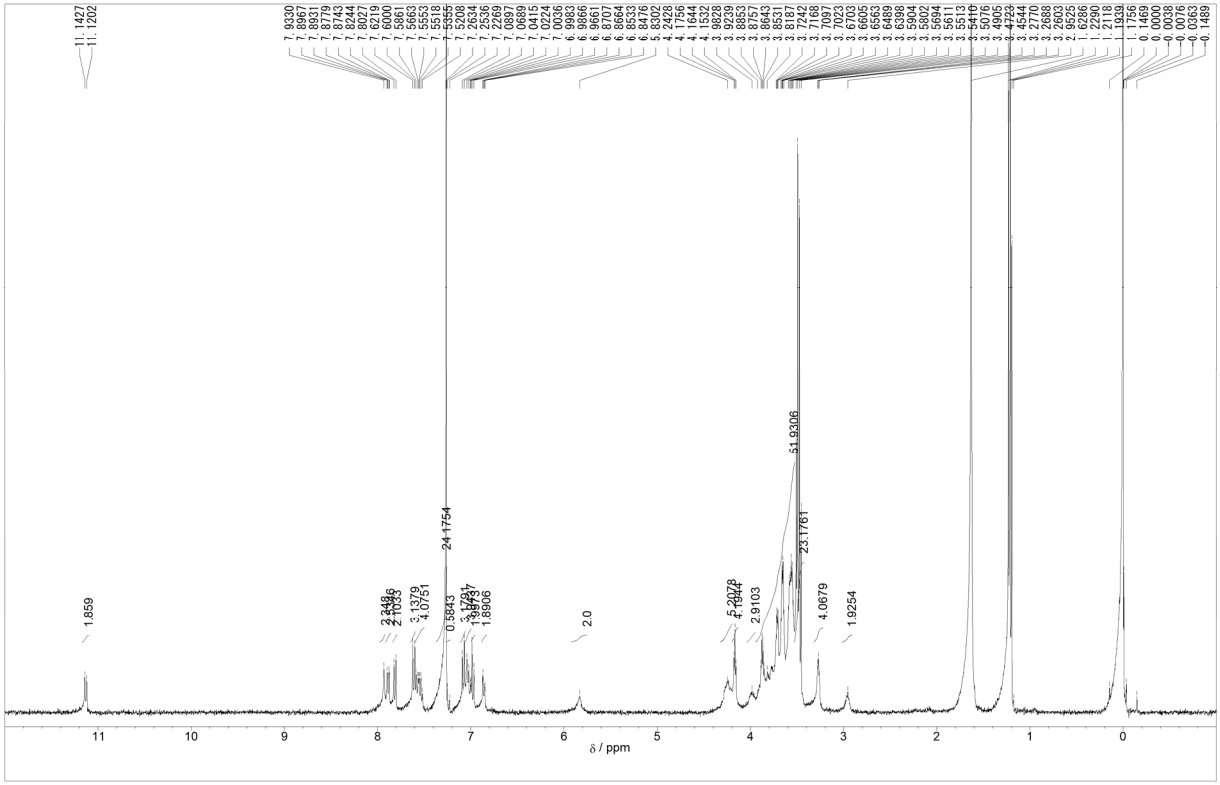

Figure S29. ^{1}H NMR spectrum of amphiphilic chiral salen complex [**L^{1b}**Zn] (400 MHz, $CDCl_3$).

4.1. Estimation of molecular cross-section areas.

The structures of the parent metallosalen compounds and [**L**^{1b}Ni] were obtained by PM6 calculations. The space-filling model of each molecule was projected onto a plane perpendicular to the approximate C_2 axis of each and the projected area was used as the cross-section of the molecules.

(a) The core structure of [**L**^{1a,b}Ni] that has no TEG or methoxy groups

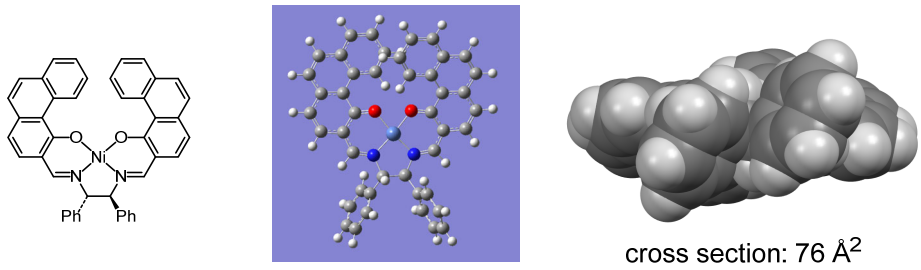

(b) The core structure of [**L**^{2a,b}Ni] that has no TEG or methoxy groups

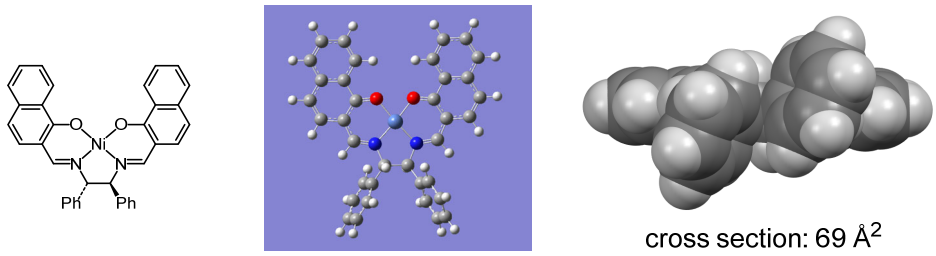

(c) The tetra-TEG derivative [**L**^{1b}Ni]

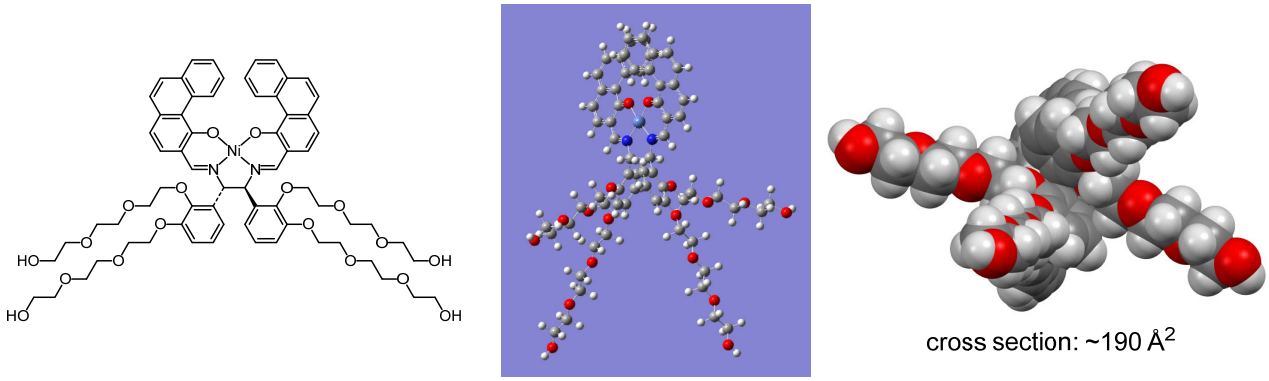

Figure S30. Calculated structures of nickel(II) complexes (PM6).

4.2. Compressibility and compression modulus of amphiphilic chiral salen nickel(II) complexes.

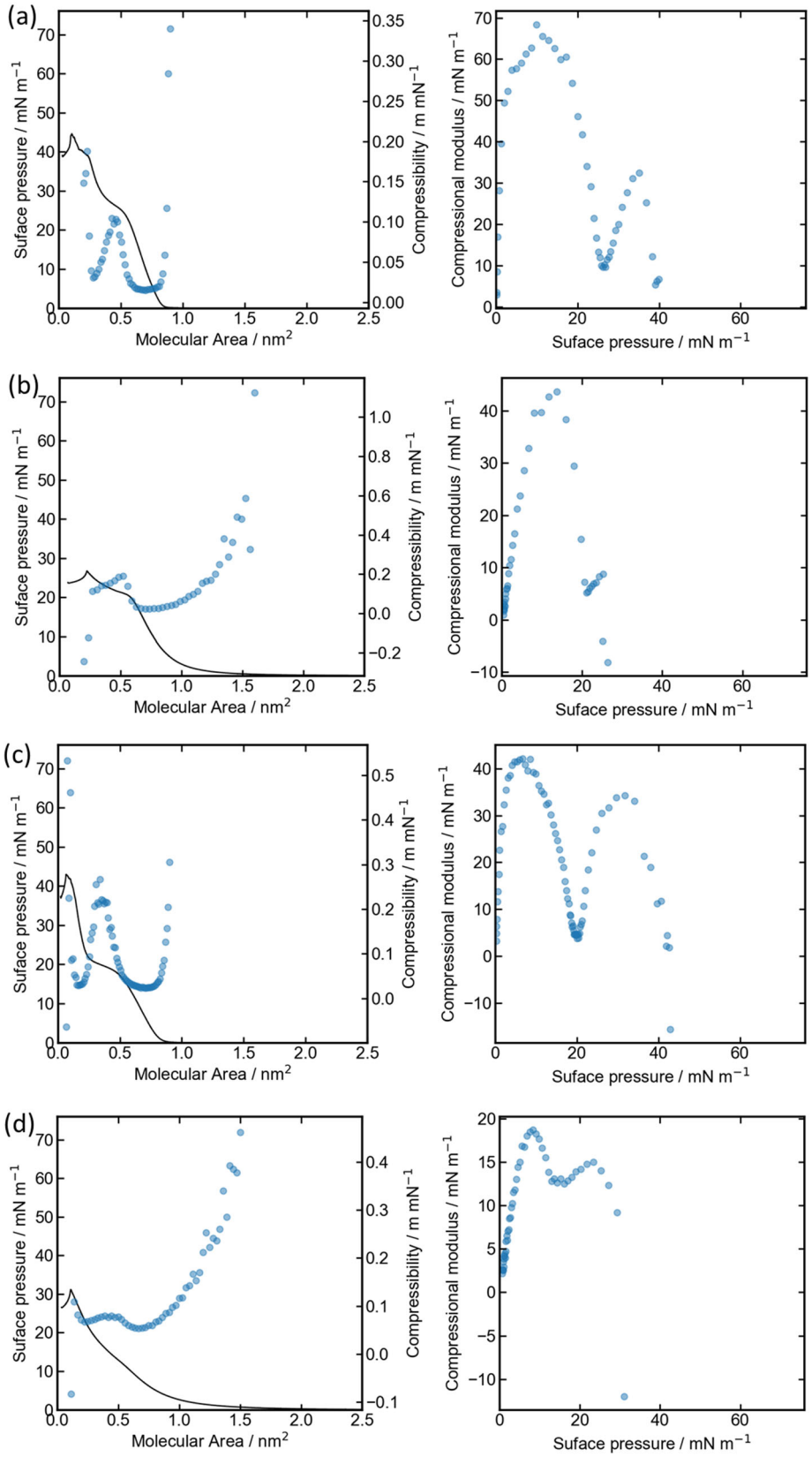

Figure S31. C_s–A isotherms of monolayers and the corresponding π–A isotherms (shown as black lines). C_s^{-1}-π curves for the monolayers. (a) [**L**$^{\mathbf{1a}}$Ni], (b) [**L**$^{\mathbf{1b}}$Ni], (c) [**L**$^{\mathbf{2a}}$Ni], and (d) [**L**$^{\mathbf{2b}}$Ni].

4.3. UV-vis absorption spectra of LB films of amphiphilic chiral salen nickel(II) complex [L^{1b}Ni].

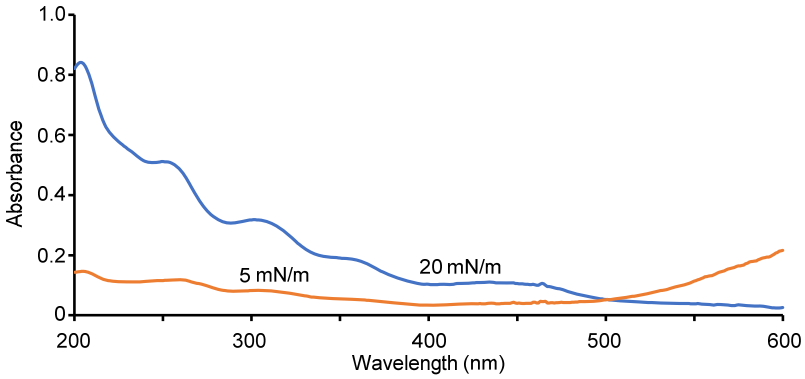

Figure S32. UV-vis absorption spectra of LB films of [**L**^{1b}Ni] after normalization.